Electronic Supplementary Material (ESI) for Materials Chemistry Frontiers.

Supplementary Information

Biomimetic Formation of Fluorapatite Nanorods in Confinement and the Opposite Effects of Additives on the Crystallization Kinetics

Meng Cai,[a,b] Haoyue Song,[a] Qihang Wang,[a] Zhaoyong Zou *,[a,b] and Zhengyi Fu *,[a,b]

a. *State Key Laboratory of Advanced Technology for Materials Synthesis and Processing, Wuhan University of Technology, Wuhan 430070, China.*
b. *Hubei Longzhong Laboratory, Xiangyang 441000, Hubei, China.*

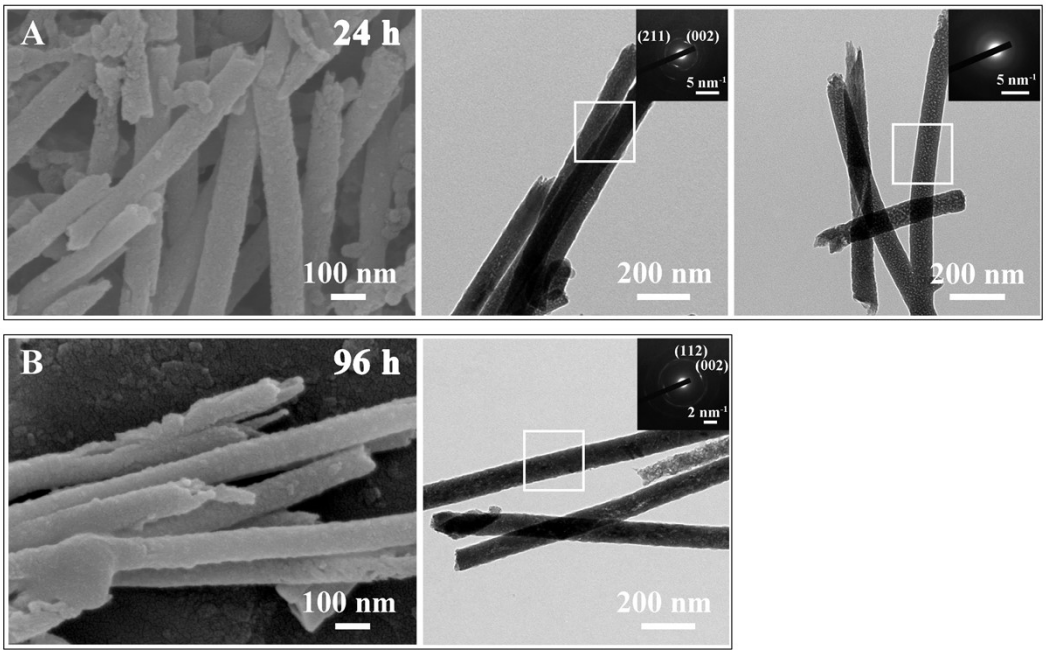

Figure S1. SEM and TEM images of FAP nanorods collected from 50 nm pores with no additive at initial [Ca^{2+}] of 10 mM after reaction for (a) 24 h and (b) 96 h. The insets in TEM images are the SAED patterns corresponding to the rectangular regions respectively.

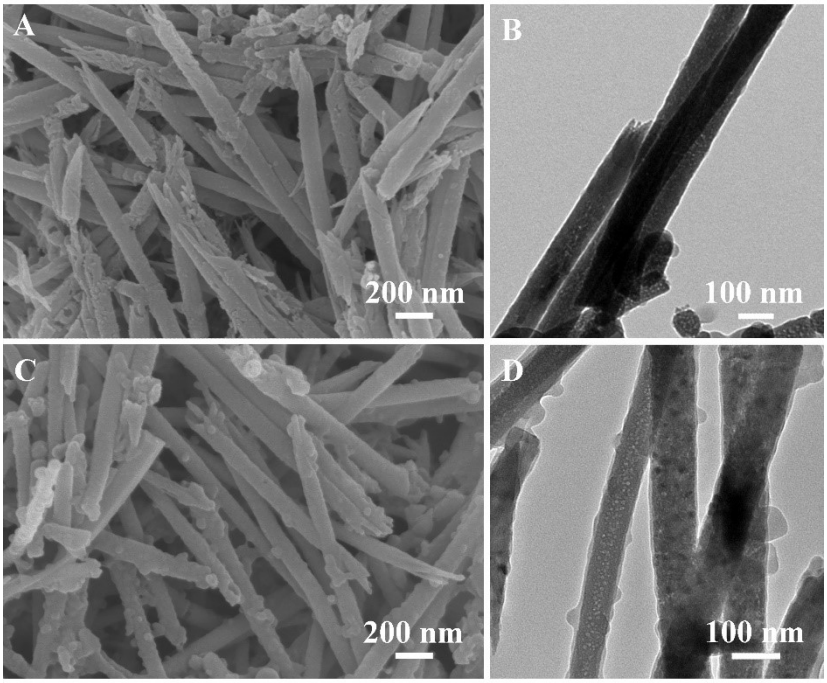

Figure S2. SEM and TEM images of FAP nanorods collected from TE membranes with pore size of 50 nm at initial [Ca^{2+}] of (A, B) 5 mM and (C, D) 20 mM with no additive after reaction for 24 h.

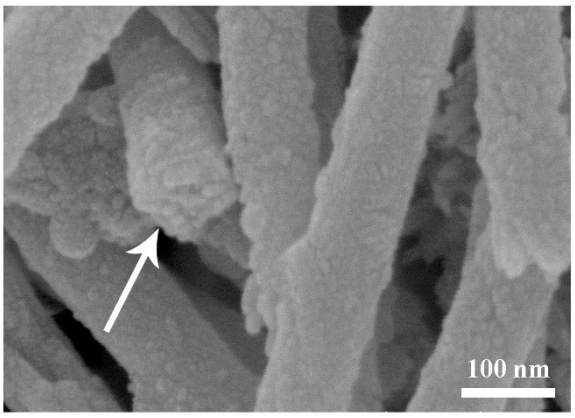

Figure S3. SEM image of fractured FAP nanorods collected from TE membranes with pore size of 50 nm at initial [Ca^{2+}] of 10 mM.

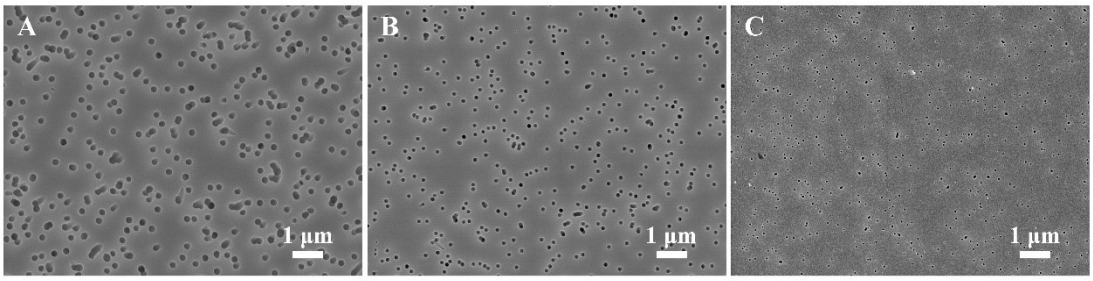

Figure S4. SEM images about the surface of polycarbonate TE membranes with different pore

diameters, showing homogeneous distribution of cylindrical pores. (A) 200 nm, (B) 100 nm and (C) 50 nm.

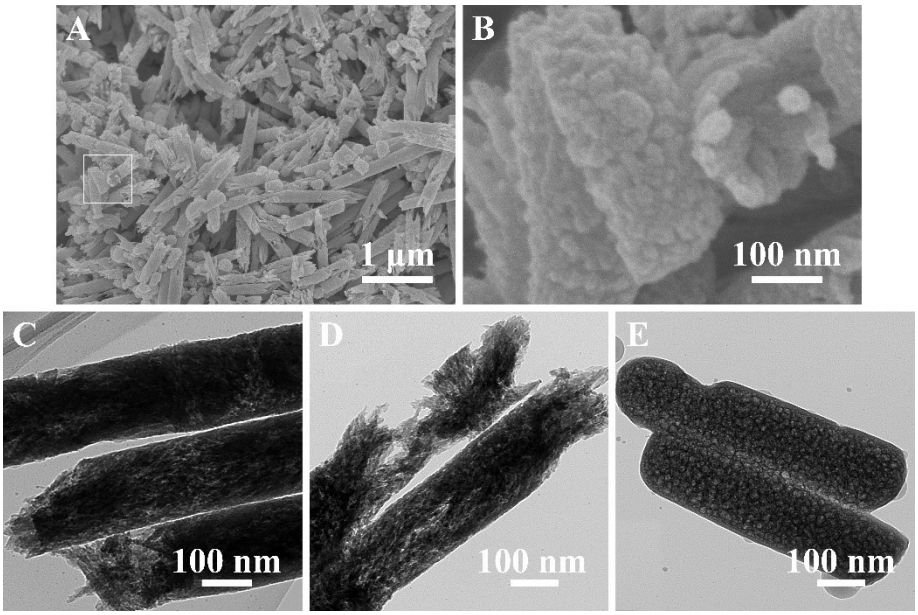

Figure S5. SEM (A-B) and TEM (C-F) images of FAP nanorods collected from 100 nm pores at $[Ca^{2+}]$ = 10 mM with no additive after reaction for 3 h. (B) High magnification images of white rectangular regions in (A). (C, D) Nanorods composed of nanocrystals which are not sensitive to electron radiation. (E) Nanorods composed of amorphous nanoparticles which are damaged by electron irradiation.

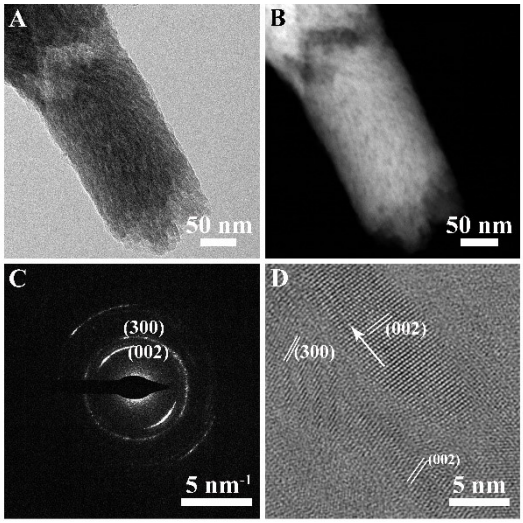

Figure S6. TEM images of a broken FAP nanorod collected from 100 nm pores with no additive at $[Ca^{2+}]$ = 10 mM after reaction for 24 h. (A-B) BF-TEM image and DF-TEM image. (C) The SAED image of (A). (D) HRTEM images of the broken port in (A).

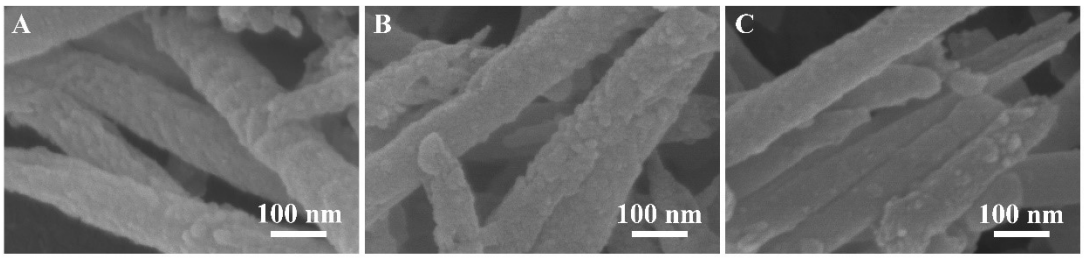

Figure S7. SEM images of FAP nanorods collected from 50 nm pores after reaction for 24h with different additives. (A) 0.5 mM Mg^{2+}, (B) 0.5 mM Sr^{2+} and (C) 20 μg/ml PAAs.

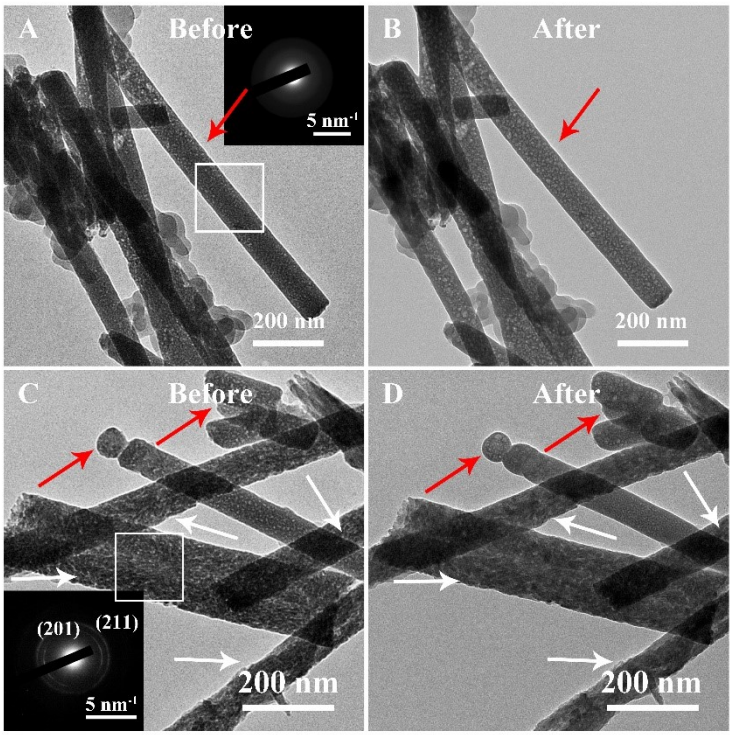

Figure S8. TEM images of FAP nanorods selected randomly from 50 nm nanopores that show the morphology changes produced by the electron beam. (A, C) Images captured as soon as possible once electron beams focus. (B, D) Images of in-situ observation after electron radiation for 1 min. The inserts in (A, C) are the SEAD patterns of corresponding white rectangular regions. The white arrows indicate crystalline FAP nanorods that are less sensitive to electron radiation while the red arrows indicate the sensitive ones.

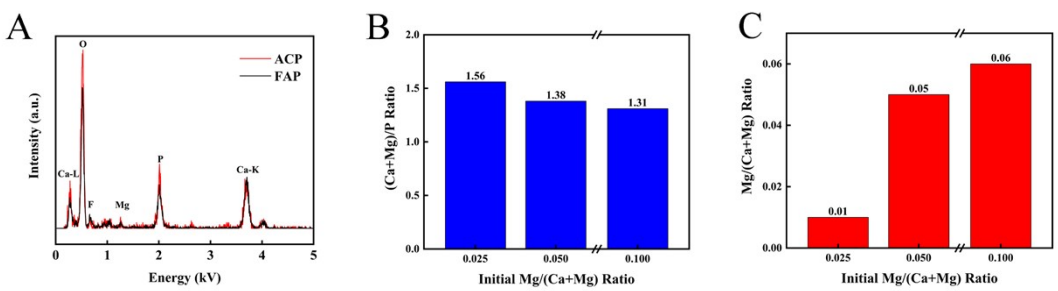

Figure S9. (A) Normalized EDS images of ACP and crystalline FAP nanorods collected from 50 nm pores at initial Mg/(Ca+Mg) = 0.1 after reaction for 24 h. (B, C) The relationships between (B) (Ca + Mg)/P ratio, (C) Mg/(Ca + Mg) ratio of the crystalline FAP nanorods and initial Mg/(Ca + Mg) ratio in solution collected from 50 nm pores after reaction for 24 h.